

Measurement of the $Z\gamma \rightarrow \nu\bar{\nu}\gamma$ Production Cross Section and Limits on Anomalous $ZZ\gamma$ and $Z\gamma\gamma$ Couplings in $p\bar{p}$ Collisions at $\sqrt{s} = 1.96$ TeV

V. M. Abazov,³⁶ B. Abbott,⁷⁴ M. Abolins,⁶⁴ B. S. Acharya,²⁹ M. Adams,⁵⁰ T. Adams,⁴⁸ E. Aguilo,⁶ M. Ahsan,⁵⁸ G. D. Alexeev,³⁶ G. Alkhazov,⁴⁰ A. Alton,^{63,*} G. Alverson,⁶² G. A. Alves,² M. Anastasoie,³⁵ L. S. Ancu,³⁵ T. Andeen,⁵² M. S. Anzelc,⁵² M. Aoki,⁴⁹ Y. Arnoud,¹⁴ M. Arov,⁵⁹ M. Arthaud,¹⁸ A. Askew,^{48,†} B. Åsman,⁴¹ O. Atramentov,⁴⁸ C. Avila,⁸ J. BackusMayes,⁸¹ F. Badaud,¹³ L. Bagby,⁴⁹ B. Baldin,⁴⁹ D. V. Bandurin,⁵⁸ P. Banerjee,²⁹ S. Banerjee,²⁹ E. Barberis,⁶² A.-F. Barfuss,¹⁵ P. Bargassa,⁷⁹ P. Baringer,⁵⁷ J. Barreto,² J. F. Bartlett,⁴⁹ U. Bassler,¹⁸ D. Bauer,⁴³ S. Beale,⁶ A. Bean,⁵⁷ M. Begalli,³ M. Biegel,⁷² C. Belanger-Champagne,⁴¹ L. Bellantoni,⁴⁹ A. Bellavance,⁴⁹ J. A. Benitez,⁶⁴ S. B. Beri,²⁷ G. Bernardi,¹⁷ R. Bernhard,²³ I. Bertram,⁴² M. Besançon,¹⁸ R. Beuselinck,⁴³ V. A. Bezzubov,³⁹ P. C. Bhat,⁴⁹ V. Bhatnagar,²⁷ G. Blazey,⁵¹ S. Blessing,⁴⁸ K. Bloom,⁶⁶ A. Boehnlein,⁴⁹ D. Boline,⁶¹ T. A. Bolton,⁵⁸ E. E. Boos,³⁸ G. Borissov,⁴² T. Bose,⁷⁶ A. Brandt,⁷⁷ R. Brock,⁶⁴ G. Brooijmans,⁶⁹ A. Bross,⁴⁹ D. Brown,¹⁹ X. B. Bu,⁷ N. J. Buchanan,⁴⁸ D. Buchholz,⁵² M. Buehler,⁸⁰ V. Buescher,²² V. Bunichev,³⁸ S. Burdin,^{42,‡} T. H. Burnett,⁸¹ C. P. Buszello,⁴³ P. Calfayan,²⁵ B. Calpas,¹⁵ S. Calvet,¹⁶ J. Cammin,⁷⁰ M. A. Carrasco-Lizarraga,³³ E. Carrera,⁴⁸ W. Carvalho,³ B. C. K. Casey,⁴⁹ H. Castilla-Valdez,³³ S. Chakrabarti,⁷¹ D. Chakraborty,⁵¹ K. M. Chan,⁵⁴ A. Chandra,⁴⁷ E. Cheu,⁴⁵ D. K. Cho,⁶¹ S. Choi,³² B. Choudhary,²⁸ L. Christofek,⁷⁶ T. Christoudias,⁴³ S. Cihangir,⁴⁹ D. Claes,⁶⁶ J. Clutter,⁵⁷ M. Cooke,⁴⁹ W. E. Cooper,⁴⁹ M. Corcoran,⁷⁹ F. Couderc,¹⁸ M.-C. Cousinou,¹⁵ S. Crépe-Renaudin,¹⁴ V. Cuplov,⁵⁸ D. Cutts,⁷⁶ M. Ćwiok,³⁰ A. Das,⁴⁵ G. Davies,⁴³ K. De,⁷⁷ S. J. de Jong,³⁵ E. De La Cruz-Burelo,³³ K. DeVaughan,⁶⁶ F. Déliot,¹⁸ M. Demarteau,⁴⁹ R. Demina,⁷⁰ D. Denisov,⁴⁹ S. P. Denisov,³⁹ S. Desai,⁴⁹ H. T. Diehl,⁴⁹ M. Diesburg,⁴⁹ A. Dominguez,⁶⁶ T. Dorland,⁸¹ A. Dubey,²⁸ L. V. Dudko,³⁸ L. Duflot,¹⁶ D. Duggan,⁴⁸ A. Duperrin,¹⁵ S. Dutt,²⁷ A. Dyshkant,⁵¹ M. Eads,⁶⁶ D. Edmunds,⁶⁴ J. Ellison,⁴⁷ V. D. Elvira,⁴⁹ Y. Enari,⁷⁶ S. Eno,⁶⁰ P. Ermolov,^{38,§} M. Escalier,¹⁵ H. Evans,⁵³ A. Evdokimov,⁷² V. N. Evdokimov,³⁹ A. V. Ferapontov,⁵⁸ T. Ferbel,^{60,70} F. Fiedler,²⁴ F. Filthaut,³⁵ W. Fisher,⁴⁹ H. E. Fisk,⁴⁹ M. Fortner,⁵¹ H. Fox,⁴² S. Fu,⁴⁹ S. Fuess,⁴⁹ T. Gadfort,⁶⁹ C. F. Galea,³⁵ A. Garcia-Bellido,⁷⁰ V. Gavrilov,³⁷ P. Gay,¹³ W. Geist,¹⁹ W. Geng,^{15,64} C. E. Gerber,⁵⁰ Y. Gershtein,^{48,†} D. Gillberg,⁶ G. Ginther,⁷⁰ B. Gómez,⁸ A. Goussiou,⁸¹ P. D. Grannis,⁷¹ H. Greenlee,⁴⁹ Z. D. Greenwood,⁵⁹ E. M. Gregores,⁴ G. Grenier,²⁰ Ph. Gris,¹³ J.-F. Grivaz,¹⁶ A. Grohsjean,²⁵ S. Grünendahl,⁴⁹ M. W. Grünwald,³⁰ F. Guo,⁷¹ J. Guo,⁷¹ G. Gutierrez,⁴⁹ P. Gutierrez,⁷⁴ A. Haas,⁶⁹ N. J. Hadley,⁶⁰ P. Haefner,²⁵ S. Hagopian,⁴⁸ J. Haley,⁶⁷ I. Hall,⁶⁴ R. E. Hall,⁴⁶ L. Han,⁷ K. Harder,⁴⁴ A. Harel,⁷⁰ J. M. Hauptman,⁵⁶ J. Hays,⁴³ T. Hebbeker,²¹ D. Hedin,⁵¹ J. G. Hegeman,³⁴ A. P. Heinson,⁴⁷ U. Heintz,⁶¹ C. Hensel,^{22,§} K. Herner,⁶³ G. Hesketh,⁶² M. D. Hildreth,⁵⁴ R. Hirosky,⁸⁰ T. Hoang,⁴⁸ J. D. Hobbs,⁷¹ B. Hoeneisen,¹² M. Hohlfield,²² S. Hossain,⁷⁴ P. Houben,³⁴ Y. Hu,⁷¹ Z. Hubacek,¹⁰ N. Huske,¹⁷ V. Hynek,⁹ I. Iashvili,⁶⁸ R. Illingworth,⁴⁹ A. S. Ito,⁴⁹ S. Jabeen,⁶¹ M. Jaffré,¹⁶ S. Jain,⁷⁴ K. Jakobs,²³ D. Jamin,¹⁵ C. Jarvis,⁶⁰ R. Jesik,⁴³ K. Johns,⁴⁵ C. Johnson,⁶⁹ M. Johnson,⁴⁹ D. Johnston,⁶⁶ A. Jonckheere,⁴⁹ P. Jonsson,⁴³ A. Juste,⁴⁹ E. Kajfasz,¹⁵ D. Karmanov,³⁸ P. A. Kasper,⁴⁹ I. Katsanos,⁶⁹ V. Kaushik,⁷⁷ R. Kehoe,⁷⁸ S. Kermiche,¹⁵ N. Khalatyan,⁴⁹ A. Khanov,⁷⁵ A. Kharchilava,⁶⁸ Y. N. Kharzheev,³⁶ D. Khatidze,⁶⁹ T. J. Kim,³¹ M. H. Kirby,⁵² M. Kirsch,²¹ B. Klima,⁴⁹ J. M. Kohli,²⁷ J.-P. Konrath,²³ A. V. Kozelov,³⁹ J. Kraus,⁶⁴ T. Kuhl,²⁴ A. Kumar,⁶⁸ A. Kupco,¹¹ T. Kurča,²⁰ V. A. Kuzmin,³⁸ J. Kvita,⁹ F. Lacroix,¹³ D. Lam,⁵⁴ S. Lammers,⁵³ G. Landsberg,⁷⁶ P. Lebrun,²⁰ W. M. Lee,⁴⁹ A. Leflat,³⁸ J. Lellouch,¹⁷ J. Li,^{77,§§} L. Li,⁴⁷ Q. Z. Li,⁴⁹ S. M. Lietti,⁵ J. K. Lim,³¹ D. Lincoln,⁴⁹ J. Linnemann,⁶⁴ V. V. Lipaev,³⁹ R. Lipton,⁴⁹ Y. Liu,⁷ Z. Liu,⁶ A. Lobodenko,⁴⁰ M. Lokajicek,¹¹ P. Love,⁴² H. J. Lubatti,⁸¹ R. Luna-Garcia,^{33,||} A. L. Lyon,⁴⁹ A. K. A. Maciel,² D. Mackin,⁷⁹ P. Mättig,²⁶ A. Magerkurth,⁶³ P. K. Mal,⁸¹ H. B. Malbouisson,³ S. Malik,⁶⁶ V. L. Malyshev,³⁶ Y. Maravin,⁵⁸ B. Martin,¹⁴ R. McCarthy,⁷¹ M. M. Meijer,³⁵ A. Melnitchouk,⁶⁵ L. Mendoza,⁸ P. G. Mercadante,⁵ M. Merkin,³⁸ K. W. Merritt,⁴⁹ A. Meyer,²¹ J. Meyer,^{22,§} J. Mitrevski,⁶⁹ R. K. Mommsen,⁴⁴ N. K. Mondal,²⁹ R. W. Moore,⁶ T. Moulik,⁵⁷ G. S. Muanza,¹⁵ M. Mulhearn,⁶⁹ O. Mundal,²² L. Mundim,³ E. Nagy,¹⁵ M. Naimuddin,⁴⁹ M. Narain,⁷⁶ H. A. Neal,⁶³ J. P. Negret,⁸ P. Neustroev,⁴⁰ H. Nilsen,²³ H. Nogima,³ S. F. Novaes,⁵ T. Nunnemann,²⁵ D. C. O'Neil,⁶ G. Obrant,⁴⁰ C. Ochando,¹⁶ D. Onoprienko,⁵⁸ J. Orduna,³³ N. Oshima,⁴⁹ N. Osman,⁴³ J. Osta,⁵⁴ R. Otec,¹⁰ G. J. Otero y Garzón,¹ M. Owen,⁴⁴ M. Padilla,⁴⁷ P. Padley,⁷⁹ M. Pangilinan,⁷⁶ N. Parashar,⁵⁵ S.-J. Park,^{22,§} S. K. Park,³¹ J. Parsons,⁶⁹ R. Partridge,⁷⁶ N. Parua,⁵³ A. Patwa,⁷² G. Pawloski,⁷⁹ B. Penning,³⁸ M. Perfilov,³⁸ K. Peters,⁴⁴ Y. Peters,²⁶ P. Pétrouff,¹⁶ R. Piegaia,¹ J. Piper,⁶⁴ M.-A. Pleier,²² P. L. M. Podesta-Lerma,^{33,||} V. M. Podstavkov,⁴⁹ Y. Pogorelov,⁵⁴ M.-E. Pol,² P. Polozov,³⁷ A. V. Popov,³⁹ C. Potter,⁶ W. L. Prado da Silva,³ S. Protopopescu,⁷² J. Qian,⁶³ A. Quadt,^{22,§} B. Quinn,⁶⁵ A. Rakitine,⁴² M. S. Rangel,² K. Ranjan,²⁸ P. N. Ratoff,⁴² P. Renkel,⁷⁸ P. Rich,⁴⁴ M. Rijssenbeek,⁷¹ I. Ripp-Baudot,¹⁹ F. Rizatdinova,⁷⁵ S. Robinson,⁴³ R. F. Rodrigues,³ M. Rominsky,⁷⁴ C. Royon,¹⁸ P. Rubinov,⁴⁹ R. Ruchti,⁵⁴ G. Safronov,³⁷ G. Sajot,¹⁴

A. Sánchez-Hernández,³³ M. P. Sanders,¹⁷ B. Sanghi,⁴⁹ G. Savage,⁴⁹ L. Sawyer,⁵⁹ T. Scanlon,⁴³ D. Schaile,²⁵
 R. D. Schamberger,⁷¹ Y. Scheglov,⁴⁰ H. Schellman,⁵² T. Schliephake,²⁶ S. Schlobohm,⁸¹ C. Schwanenberger,⁴⁴
 R. Schwienhorst,⁶⁴ J. Sekaric,⁴⁸ H. Severini,⁷⁴ E. Shabalina,⁵⁰ M. Shamim,⁵⁸ V. Shary,¹⁸ A. A. Shchukin,³⁹
 R. K. Shivpuri,²⁸ V. Siccaldi,¹⁹ V. Simak,¹⁰ V. Sirotenko,⁴⁹ P. Skubic,⁷⁴ P. Slattery,⁷⁰ D. Smirnov,⁵⁴ G. R. Snow,⁶⁶
 J. Snow,⁷³ S. Snyder,⁷² S. Söldner-Rembold,⁴⁴ L. Sonnenschein,²¹ A. Sopczak,⁴² M. Sosebee,⁷⁷ K. Soustruznik,⁹
 B. Spurlock,⁷⁷ J. Stark,¹⁴ V. Stolin,³⁷ D. A. Stoyanova,³⁹ J. Strandberg,⁶³ S. Strandberg,⁴¹ M. A. Strang,⁶⁸ E. Strauss,⁷¹
 M. Strauss,⁷⁴ R. Ströhmer,²⁵ D. Strom,⁵² L. Stutte,⁴⁹ S. Sumowidagdo,⁴⁸ P. Svoisky,³⁵ A. Tanasijczuk,¹ W. Taylor,⁶
 B. Tiller,²⁵ F. Tissandier,¹³ M. Titov,¹⁸ V. V. Tokmenin,³⁶ I. Torchiani,²³ D. Tsybychev,⁷¹ B. Tuchming,¹⁸ C. Tully,⁶⁷
 P. M. Tuts,⁶⁹ R. Unalan,⁶⁴ L. Uvarov,⁴⁰ S. Uvarov,⁴⁰ S. Uzunyan,⁵¹ B. Vachon,⁶ P. J. van den Berg,³⁴ R. Van Kooten,⁵³
 W. M. van Leeuwen,³⁴ N. Varelas,⁵⁰ E. W. Varnes,⁴⁵ I. A. Vasilyev,³⁹ P. Verdier,²⁰ L. S. Vertogradov,³⁶ M. Verzocchi,⁴⁹
 D. Vilanova,¹⁸ P. Vint,⁴³ P. Vokac,¹⁰ M. Voutilainen,^{66,**} R. Wagner,⁶⁷ H. D. Wahl,⁴⁸ M. H. L. S. Wang,⁴⁹ J. Warchol,⁵⁴
 G. Watts,⁸¹ M. Wayne,⁵⁴ G. Weber,²⁴ M. Weber,^{49,††} L. Welty-Rieger,⁵³ A. Wenger,^{23,‡‡} M. Wetstein,⁶⁰ A. White,⁷⁷
 D. Wicke,²⁶ M. R. J. Williams,⁴² G. W. Wilson,⁵⁷ S. J. Wimpenny,⁴⁷ M. Wobisch,⁵⁹ D. R. Wood,⁶² T. R. Wyatt,⁴⁴ Y. Xie,⁷⁶
 C. Xu,⁶³ S. Yacoub,⁵² R. Yamada,⁴⁹ W.-C. Yang,⁴⁴ T. Yasuda,⁴⁹ Y. A. Yatsunenko,³⁶ Z. Ye,⁴⁹ H. Yin,⁷ K. Yip,⁷²
 H. D. Yoo,⁷⁶ S. W. Youn,⁵² J. Yu,⁷⁷ C. Zeitnitz,²⁶ S. Zelitch,⁸⁰ T. Zhao,⁸¹ B. Zhou,⁶³ J. Zhu,⁷¹ M. Zielinski,⁷⁰
 D. Zieminska,⁵³ L. Zivkovic,⁶⁹ V. Zutshi,⁵¹ and E. G. Zverev³⁸

(D0 Collaboration)

¹Universidad de Buenos Aires, Buenos Aires, Argentina²LAFEX, Centro Brasileiro de Pesquisas Físicas, Rio de Janeiro, Brazil³Universidade do Estado do Rio de Janeiro, Rio de Janeiro, Brazil⁴Universidade Federal do ABC, Santo André, Brazil⁵Instituto de Física Teórica, Universidade Estadual Paulista, São Paulo, Brazil⁶University of Alberta, Edmonton, Alberta, Canada,

Simon Fraser University, Burnaby, British Columbia, Canada,

York University, Toronto, Ontario, Canada,

and McGill University, Montreal, Quebec, Canada

⁷University of Science and Technology of China, Hefei, People's Republic of China⁸Universidad de los Andes, Bogotá, Colombia⁹Center for Particle Physics, Charles University, Prague, Czech Republic¹⁰Czech Technical University in Prague, Prague, Czech Republic¹¹Center for Particle Physics, Institute of Physics, Academy of Sciences of the Czech Republic, Prague, Czech Republic¹²Universidad San Francisco de Quito, Quito, Ecuador¹³LPC, Université Blaise Pascal, CNRS/IN2P3, Clermont, France¹⁴LPSC, Université Joseph Fourier Grenoble I, CNRS/IN2P3, Institut National Polytechnique de Grenoble, Grenoble, France¹⁵CPPM, Aix-Marseille Université, CNRS/IN2P3, Marseille, France¹⁶LAL, Université Paris-Sud, IN2P3/CNRS, Orsay, France¹⁷LPNHE, IN2P3/CNRS, Universités Paris VI and VII, Paris, France¹⁸CEA, Ifu, SPP, Saclay, France¹⁹IPHC, Université de Strasbourg, CNRS/IN2P3, Strasbourg, France²⁰IPNL, Université Lyon I, CNRS/IN2P3, Villeurbanne, France

and Université de Lyon, Lyon, France

²¹III. Physikalisches Institut A, RWTH Aachen University, Aachen, Germany²²Physikalisches Institut, Universität Bonn, Bonn, Germany²³Physikalisches Institut, Universität Freiburg, Freiburg, Germany²⁴Institut für Physik, Universität Mainz, Mainz, Germany²⁵Ludwig-Maximilians-Universität München, München, Germany²⁶Fachbereich Physik, University of Wuppertal, Wuppertal, Germany²⁷Panjab University, Chandigarh, India²⁸Delhi University, Delhi, India²⁹Tata Institute of Fundamental Research, Mumbai, India³⁰University College Dublin, Dublin, Ireland³¹Korea Detector Laboratory, Korea University, Seoul, Korea³²SungKyunKwan University, Suwon, Korea³³CINVESTAV, Mexico City, Mexico³⁴FOM-Institute NIKHEF and University of Amsterdam/NIKHEF, Amsterdam, The Netherlands

- ³⁵Radboud University Nijmegen/NIKHEF, Nijmegen, The Netherlands
³⁶Joint Institute for Nuclear Research, Dubna, Russia
³⁷Institute for Theoretical and Experimental Physics, Moscow, Russia
³⁸Moscow State University, Moscow, Russia
³⁹Institute for High Energy Physics, Protvino, Russia
⁴⁰Petersburg Nuclear Physics Institute, St. Petersburg, Russia
⁴¹Stockholm University, Stockholm, Sweden,
and Uppsala University, Uppsala, Sweden
⁴²Lancaster University, Lancaster, United Kingdom
⁴³Imperial College, London, United Kingdom
⁴⁴University of Manchester, Manchester, United Kingdom
⁴⁵University of Arizona, Tucson, Arizona 85721, USA
⁴⁶California State University, Fresno, California 93740, USA
⁴⁷University of California, Riverside, California 92521, USA
⁴⁸Florida State University, Tallahassee, Florida 32306, USA
⁴⁹Fermi National Accelerator Laboratory, Batavia, Illinois 60510, USA
⁵⁰University of Illinois at Chicago, Chicago, Illinois 60607, USA
⁵¹Northern Illinois University, DeKalb, Illinois 60115, USA
⁵²Northwestern University, Evanston, Illinois 60208, USA
⁵³Indiana University, Bloomington, Indiana 47405, USA
⁵⁴University of Notre Dame, Notre Dame, Indiana 46556, USA
⁵⁵Purdue University Calumet, Hammond, Indiana 46323, USA
⁵⁶Iowa State University, Ames, Iowa 50011, USA
⁵⁷University of Kansas, Lawrence, Kansas 66045, USA
⁵⁸Kansas State University, Manhattan, Kansas 66506, USA
⁵⁹Louisiana Tech University, Ruston, Louisiana 71272, USA
⁶⁰University of Maryland, College Park, Maryland 20742, USA
⁶¹Boston University, Boston, Massachusetts 02215, USA
⁶²Northeastern University, Boston, Massachusetts 02115, USA
⁶³University of Michigan, Ann Arbor, Michigan 48109, USA
⁶⁴Michigan State University, East Lansing, Michigan 48824, USA
⁶⁵University of Mississippi, University, Mississippi 38677, USA
⁶⁶University of Nebraska, Lincoln, Nebraska 68588, USA
⁶⁷Princeton University, Princeton, New Jersey 08544, USA
⁶⁸State University of New York, Buffalo, New York 14260, USA
⁶⁹Columbia University, New York, New York 10027, USA
⁷⁰University of Rochester, Rochester, New York 14627, USA
⁷¹State University of New York, Stony Brook, New York 11794, USA
⁷²Brookhaven National Laboratory, Upton, New York 11973, USA
⁷³Langston University, Langston, Oklahoma 73050, USA
⁷⁴University of Oklahoma, Norman, Oklahoma 73019, USA
⁷⁵Oklahoma State University, Stillwater, Oklahoma 74078, USA
⁷⁶Brown University, Providence, Rhode Island 02912, USA
⁷⁷University of Texas, Arlington, Texas 76019, USA
⁷⁸Southern Methodist University, Dallas, Texas 75275, USA
⁷⁹Rice University, Houston, Texas 77005, USA
⁸⁰University of Virginia, Charlottesville, Virginia 22901, USA
⁸¹University of Washington, Seattle, Washington 98195, USA
(Received 12 February 2009; published 22 May 2009)

We present the first observation of the $Z\gamma \rightarrow \nu\bar{\nu}\gamma$ process at the Fermilab Tevatron at 5.1 standard deviations significance, based on 3.6 fb^{-1} of integrated luminosity collected with the D0 detector at the Fermilab Tevatron $p\bar{p}$ Collider at $\sqrt{s} = 1.96 \text{ TeV}$. The measured $Z\gamma$ production cross section multiplied by the branching fraction of $Z \rightarrow \nu\bar{\nu}$ is $32 \pm 9(\text{stat} + \text{syst}) \pm 2(\text{lumi}) \text{ fb}$ for the photon $E_T > 90 \text{ GeV}$. It is in agreement with the standard model prediction of $39 \pm 4 \text{ fb}$. We set limits on anomalous trilinear $Z\gamma\gamma$ and $ZZ\gamma$ gauge boson couplings, most of which are the most restrictive to date.

The standard model (SM) of electroweak interactions is described by the non-Abelian gauge group $SU(2) \times U(1)$. The symmetry transformations of the group allow interactions involving three gauge bosons (γ , W , and Z) through trilinear gauge boson couplings. However, the SM forbids such vertices for the photon and the Z boson at the lowest “tree” level; i.e., the values of the $Z\gamma\gamma$ and $ZZ\gamma$ couplings vanish. The cross section for the SM $Z\gamma$ production is very small. However, the presence of nonzero (*anomalous*) $Z\gamma\gamma$ and $ZZ\gamma$ couplings can enhance the yields, especially at higher values of the photon transverse energy (E_T). As we are marginally sensitive to one-loop SM contributions [1,2] to these vertices, observation of an anomalously high $Z\gamma$ production rate could, therefore, indicate the presence of new physics.

To preserve S -matrix unitarity, the anomalous couplings must vanish at high center-of-mass energies. Hence, the dependence on the center-of-mass energy has to be included in the definition of such couplings. This can be done by using a set of eight complex parameters h_i^V ($i = 1, \dots, 4$; $V = Z, \gamma$) of the form $h_i^V = h_{i0}^V / (1 + \hat{s} / \Lambda^2)^n$ [3]. Here \hat{s} is the square of the center-of-mass energy in the partonic collision, Λ is a scale related to the mass of the new physics responsible for anomalous $Z\gamma$ production, and h_{i0}^V is the low energy approximation of the coupling. Following Ref. [3], we will use $n = 3$ for h_1^V and h_3^V and $n = 4$ for h_2^V and h_4^V . This choice of n guarantees the preservation of partial-wave unitarity and makes the vertex function terms proportional to h_1^V and h_3^V behave in the same way as terms proportional to h_2^V and h_4^V at high energies. Couplings h_{10}^V and h_{20}^V (h_{30}^V and h_{40}^V) are CP -violating (CP -conserving). In this Letter, we set limits on the size of the real parts of the anomalous couplings: $\text{Re}(h_{i0}^V)$, which we refer to as ATGC in the following.

In the past, studies of $Z\gamma$ production have been performed by the CDF [4] and D0 [5,6] Collaborations at the Tevatron Collider, as well as at the CERN LEP Collider by the DELPHI [7], L3 [8], and OPAL [9] Collaborations. The most recent combination of LEP results can be found in Ref. [10].

The D0 detector [11] consists of a central-tracking system, liquid-argon or uranium calorimeters, and a muon system. The tracking system comprises a silicon microstrip tracker and a central fiber tracker, both located within a ≈ 2 T superconducting solenoid, and provides tracking and vertexing up to pseudorapidities [12] of $|\eta| \approx 3.0$ and $|\eta| \approx 2.5$, respectively. The central (CPS) and forward preshower detectors are located between the superconducting coil and the calorimeters and consist of three and four layers of scintillator strips, respectively. The liquid-argon or uranium calorimeter is divided into a central calorimeter and two end calorimeters (ECs), covering pseudorapidities up to $|\eta| \approx 1.1$ and $|\eta| \approx 4.2$, respectively. The calorimeters are segmented into an electromagnetic section (EM), comprised of four layers, and a hadronic section, divided

longitudinally into fine and coarse sections. The calorimeter is followed by the muon system, consisting of three layers of tracking detectors and scintillation trigger counters and a 1.8 T iron toroidal magnet located between the two innermost layers. The muon system provides coverage to $|\eta| \approx 2$. Arrays of plastic scintillators in front of the EC cryostats are used to measure the luminosity.

Data for this analysis were collected with the D0 detector in the period from 2002 to 2008 and correspond to an integrated luminosity of 3.6 fb^{-1} after the application of data-quality and trigger requirements. Events must satisfy a trigger from a set of high- E_T single EM-cluster triggers, which are $(99 \pm 1)\%$ efficient for photons of $E_T > 90 \text{ GeV}$.

Photons are identified as calorimeter clusters with at least 95% of their energy deposited in the EM calorimeter, with transverse and longitudinal distributions consistent with those of a photon, and spatially isolated in the calorimeter and in the tracker. A cluster is isolated in the calorimeter if the isolation variable $I = [E_{\text{tot}}(0.4) - E_{\text{EM}}(0.2)] / E_{\text{EM}}(0.2) < 0.07$. Here $E_{\text{tot}}(0.4)$ is the total energy (corrected for the contribution from multiple $p\bar{p}$ interactions) deposited in a calorimeter cone of radius $\mathcal{R} = \sqrt{(\Delta\eta)^2 + (\Delta\phi)^2} = 0.4$, and $E_{\text{EM}}(0.2)$ is the EM energy in a cone of radius $\mathcal{R} = 0.2$. The track isolation variable, defined as the scalar sum of the transverse momenta of all tracks that originate from the interaction vertex in an annulus of $0.05 < \mathcal{R} < 0.4$ around the cluster, must be less than 2 GeV.

We obtain the photon sample by selecting events with a single photon candidate of $E_T > 90 \text{ GeV}$ and $|\eta| < 1.1$ and require a missing transverse energy in the event of $\cancel{E}_T > 70 \text{ GeV}$, which effectively suppresses the multijet background. The \cancel{E}_T is computed as the negative vector sum of the E_T of calorimeter cells and corrected for the transverse momentum of reconstructed muons and the energy corrections to reconstructed electrons and jets. To minimize large \cancel{E}_T from mismeasurement of jet energy, we reject events with jets with $E_T > 15 \text{ GeV}$. We also reject events containing reconstructed muons and events with cosmic-ray muons identified through a timing of their signal in the muon scintillators. Events with additional EM objects with $E_T > 15 \text{ GeV}$ are rejected. To suppress W boson decays into leptons, events with reconstructed high- p_T tracks are removed. To reduce the copious non-collision background (events in which muons from the beam halo or cosmic rays undergo bremsstrahlung and produce energetic photons), we use a pointing algorithm [13], exploiting the transverse and longitudinal energy distribution in the EM calorimeter and CPS. For an EM shower, this algorithm predicts the z coordinate of the production vertex (z_{EM}) along the beam direction and the distance of closest approach (DCA) [14] by fitting a straight line to the energy-weighted position of the photon energy clusters in all four layers of the EM calorimeter and

the position of the CPS cluster that is associated with the EM cluster. We require $|z_{EM} - z_V| < 10$ cm, where z_V is the z coordinate of the chosen reconstructed vertex. In about 92% of all cases, no correction is applied, since the $Z\gamma$ has been produced at this vertex. For the remaining cases, we recalculate the kinematic variables with respect to the chosen vertex. The systematic uncertainty due to the choice of the primary vertex is negligible. The selection criteria depend on the instantaneous luminosity and were optimized separately for two data sets: 2002–2006 and 2006–2008. The total selection efficiency is about 29% (22%) for the photon $E_T > 90$ GeV for the first (second) data set.

Following the procedure described in Ref. [15], we estimate the fraction of noncollision and W/Z events with misidentified jets backgrounds in the final candidate events by fitting their DCA distribution to a linear sum of three DCA templates. These templates are a template resembling the signal, a noncollision template, and a misidentified jets template. The efficiency for signal photons to have $DCA < 4$ cm is about 96%, whereas only about 35% for the noncollision background. We, therefore, restrict the analysis to this DCA region.

Other backgrounds to the $\gamma + \cancel{E}_T$ signal arise from electroweak processes such as $W \rightarrow e\nu$, where the electron is misidentified as a photon due to inefficiency of the tracker or hard bremsstrahlung, and $W\gamma$, where the lepton from the W boson decay is not reconstructed.

The $W \rightarrow e\nu$ background is estimated using a sample of isolated electrons. We apply the same kinematic requirements as in the photon sample and scale the remaining number of events by the measured rate of electron-photon misidentification. The $W\gamma$ background is estimated using a sample of Monte Carlo (MC) events generated with PYTHIA [16]. These events are passed through a detector simulation chain based on the GEANT package [17] and reconstructed using the same software as used for data. After imposing the same selection requirements as for the photon sample, scale factors are applied to correct for differences between simulation and data. The summary of backgrounds is shown in Table I. The relative contribution of the back-

grounds to the number of candidate events is about 26% (43%) for the first (second) data set.

After applying all selection criteria, we observe 51 candidate events with a predicted background of $17.3 \pm 0.6(\text{stat}) \pm 2.3(\text{syst})$ events. To estimate the total acceptance of the event selection requirements, we use MC samples produced with a leading-order (LO) $Z\gamma$ generator [3] using CTEQ6L1 (LO with LO α_s) parton distribution functions (PDFs) [18], passed through a parameterized simulation of the D0 detector. The next-to-leading-order (NLO) QCD corrections arising from soft gluon radiation and virtual one-loop corrections are taken into account through the adjustment of the photon E_T spectrum using a K factor, estimated using a NLO $Z\gamma$ event generator [19] and the CTEQ6M PDFs [18]. As we require no jets with $E_T > 15$ GeV to be present in the final state, the NLO corrections, integrated over the photon E_T range after the photon $E_T > 90$ GeV requirement, are $\approx 2\%$ or smaller for both the SM and anomalous $Z\gamma$ production. The NLO corrections distribution is fitted with a smooth function, with an uncertainty of $\approx 5\%$ arising from the fit. The uncertainty on the K factor from the jet energy scale and resolution is estimated to be $\approx 3\%$. Based on this simulation, the expected number of events from the SM signal is estimated to be 33.7 ± 3.4 events. The number of observed events (N_{obs}) and the number of predicted events ($N_{\nu\bar{\nu}\gamma}^{\text{SM}}$) are summarized in Table I.

The $Z\gamma$ production cross section multiplied by the branching fraction of $Z \rightarrow \nu\bar{\nu}$ is measured to be $32 \pm 9(\text{stat} + \text{syst}) \pm 2(\text{lumi})$ fb for the photon $E_T > 90$ GeV, which is in good agreement with the NLO cross section of 39 ± 4 fb [19]. This measurement results from the combination of individual cross section measurements in the two separate data sets considered, using the best linear unbiased estimate method [20]. Each individual measurement is consistent with the theoretical predictions within uncertainties. The main contribution to the total uncertainty on the measured cross section is the statistical uncertainty on the small number of events in the final sample and is a factor of 4–5 larger than the individual systematic uncertainties on photon identification, choice of PDFs, and kinematic criteria. The uncertainty on the theoretical cross section comes mainly from the choice of PDF (7%) and estimation of the NLO K factor (5.5%). To estimate the statistical significance of the measured cross section, we perform 10^8 background-only pseudoexperiments and calculate the p value as the fraction of pseudoexperiments with an estimated cross section above the measured one. This probability is found to be 3.1×10^{-7} , which corresponds to a statistical significance of 5.1 standard deviations (s.d.), making this the first observation of the $Z\gamma \rightarrow \nu\bar{\nu}\gamma$ process at the Tevatron.

To set limits on the ATGC, we compare the photon E_T spectrum in data with that from the sum of expected $Z\gamma$ signal [3,19] and the background (see Fig. 1) for each pair

TABLE I. Summary of background estimates and the number of observed and SM predicted events. The numbers represent a combination of two separate data sets with different profiles of the instantaneous luminosity.

	Number of events
$W \rightarrow e\nu$	$9.67 \pm 0.30(\text{stat}) \pm 0.48(\text{syst})$
Noncollision	$5.33 \pm 0.39(\text{stat}) \pm 1.91(\text{syst})$
$W/Z + \text{jet}$	$1.37 \pm 0.26(\text{stat}) \pm 0.91(\text{syst})$
$W\gamma$	$0.90 \pm 0.07(\text{stat}) \pm 0.12(\text{syst})$
Total background	$17.3 \pm 0.6(\text{stat}) \pm 2.3(\text{syst})$
$N_{\nu\bar{\nu}\gamma}^{\text{SM}}$	33.7 ± 3.4
N_{obs}	51

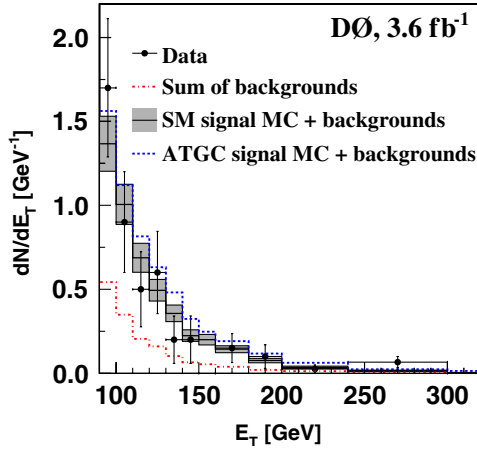


FIG. 1 (color online). Photon E_T spectrum in data (solid circles), sum of backgrounds (dashed-dotted line), and sum of the MC signal and background for the SM prediction (solid line) and for the ATGC prediction with $h_{30}^\gamma = 0.09$ and $h_{40}^\gamma = 0.005$ (dashed line). The shaded band corresponds to the ± 1 s.d. total uncertainty on the predicted sum of the SM signal and background.

of couplings for a grid in which h_{30}^V runs from -0.12 to 0.12 with a step of 0.01 , and h_{40}^V varies from -0.08 to 0.08 with a step of 0.001 . The MC samples are generated with the LO $Z\gamma$ generator (corrected for the NLO effects with an E_T -dependent K factor [19]) for the form-factor scale $\Lambda = 1.5$ TeV.

We use the binned likelihood method [21] with the likelihood calculated in each bin of the photon E_T distribution assuming Poisson statistics for the data and the predicted ATGC signal and Gaussian distributions for the background uncertainties and for all systematic uncertainties, including the luminosity. To set limits on any individual ATGC at the 95% confidence level (C.L.), we set the other anomalous couplings to zero. The resulting limits in the neutrino channel alone are $|h_{30}^\gamma| < 0.036$, $|h_{40}^\gamma| < 0.0019$ and $|h_{30}^Z| < 0.035$, $|h_{40}^Z| < 0.0019$. To further improve the sensitivity, we generate the $Z\gamma \rightarrow \ell\bar{\nu}\gamma$ ($\ell = e, \mu$) MC samples for these couplings and $\Lambda = 1.5$ TeV and set limits on ATGC for the 1 fb^{-1} data sample used in the previous $Z\gamma$ analysis [6]. The combination of all three channels yields the most stringent limits on the ATGC set at a hadron collider to date: $|h_{30}^\gamma| < 0.033$, $|h_{40}^\gamma| < 0.0017$ and $|h_{30}^Z| < 0.033$, $|h_{40}^Z| < 0.0017$. This is roughly a factor of 3 improvement over the results published in Ref. [6]. The limits on the h_{30}^Z , h_{40}^Z , and h_{40}^γ couplings improve on the constraints from LEP2 and are the most restrictive to date. The limits on the CP -violating couplings h_{10}^V and h_{20}^V are, within the precision of this measurement, the same as the limits on h_{30}^V and h_{40}^V , respectively. Hence, we can constrain the strength of the couplings but not the phase. As the described method is sensitive only to the magnitude and the relative sign between couplings, the one- and two-dimensional limits are symmetric with respect to the SM

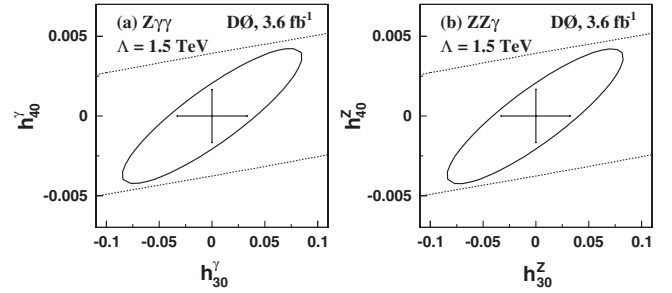


FIG. 2. Two-dimensional bounds (ellipses) at 95% C.L. on CP -conserving (a) $Z\gamma\gamma$ and (b) $ZZ\gamma$ couplings. The crosses represent the one-dimensional bounds at the 95% C.L. setting all other couplings to zero. The dashed lines indicate the unitarity limits for $\Lambda = 1.5$ TeV.

coupling under simultaneous exchange of all signs. The 95% C.L. one-dimensional limits and two-dimensional contours are shown in Figs. 2(a) and 2(b) for the CP -conserving $Z\gamma\gamma$ and $ZZ\gamma$ couplings, respectively.

In summary, we observe 51 $\nu\bar{\nu}\gamma$ candidates with $17.3 \pm 0.6(\text{stat}) \pm 2.3(\text{syst})$ background events using 3.6 fb^{-1} of data collected with the D0 detector at the Tevatron. We measure the most precise $Z\gamma \rightarrow \nu\bar{\nu}\gamma$ production cross section to date at a hadron collider of $32 \pm 9(\text{stat} + \text{syst}) \pm 2(\text{lumi}) \text{ fb}$ for the photon $E_T > 90$ GeV, in agreement with the SM prediction of $39 \pm 4 \text{ fb}$ [19]. The statistical significance of this measurement is 5.1 s.d., making it the first observation of the $Z\gamma \rightarrow \nu\bar{\nu}\gamma$ process at the Tevatron. We set the following limits on the real parts of the anomalous trilinear gauge couplings at the 95% C.L.: $|h_{30}^\gamma| < 0.033$, $|h_{40}^\gamma| < 0.0017$ and $|h_{30}^Z| < 0.033$, $|h_{40}^Z| < 0.0017$. Most of these limits are the most restrictive to date. These limits approach the range of expectations for the contributions due to one-loop diagrams in the SM [1,2].

We thank the staffs at Fermilab and collaborating institutions and acknowledge support from the DOE and NSF (USA); CEA and CNRS/IN2P3 (France); FASI, Rosatom, and RFBR (Russia); CNPq, FAPERJ, FAPESP, and FUNDUNESP (Brazil); DAE and DST (India); Colciencias (Colombia); CONACyT (Mexico); KRF and KOSEF (Korea); CONICET and UBACyT (Argentina); FOM (The Netherlands); STFC (United Kingdom); MSMT and GACR (Czech Republic); CRC Program, CFI, NSERC, and WestGrid Project (Canada); BMBF and DFG (Germany); SFI (Ireland); The Swedish Research Council (Sweden); CAS and CNSF (China); and the Alexander von Humboldt Foundation (Germany).

*Visitor from Augustana College, Sioux Falls, SD, USA.
[†]Visitor from Rutgers University, Piscataway, NJ, USA.
[‡]Visitor from The University of Liverpool, Liverpool, United Kingdom.

- [§]Visitor from II. Physikalisches Institut, Georg-August-University, Göttingen, Germany.
- ^{||}Visitor from Centro de Investigacion en Computacion - IPN, Mexico City, Mexico.
- [¶]Visitor from ECFM, Universidad Autonoma de Sinaloa, Culiacán, Mexico.
- ^{**}Visitor from Helsinki Institute of Physics, Helsinki, Finland.
- ^{††}Visitor from Universität Bern, Bern, Switzerland.
- ^{‡‡}Visitor from Universität Zürich, Zürich, Switzerland.
- ^{§§}Deceased.
- [1] G. J. Gounaris, J. Layssac, and F. M. Renard, *Phys. Rev. D* **67**, 013012 (2003).
- [2] D. Choudhury *et al.*, *Int. J. Mod. Phys. A* **16**, 4891 (2001).
- [3] U. Baur and E. Berger, *Phys. Rev. D* **47**, 4889 (1993).
- [4] D. Acosta *et al.* (CDF Collaboration), *Phys. Rev. Lett.* **94**, 041803 (2005); F. Abe *et al.* (CDF Collaboration), *Phys. Rev. Lett.* **74**, 1941 (1995).
- [5] S. Abachi *et al.* (D0 Collaboration), *Phys. Rev. Lett.* **75**, 1028 (1995); S. Abachi *et al.* (D0 Collaboration), *Phys. Rev. Lett.* **78**, 3640 (1997); B. Abbott *et al.* (D0 Collaboration), *Phys. Rev. D* **57**, R3817 (1998); V. Abazov *et al.* (D0 Collaboration), *Phys. Rev. Lett.* **95**, 051802 (2005).
- [6] V. Abazov *et al.* (D0 Collaboration), *Phys. Lett. B* **653**, 378 (2007).
- [7] J. Abdallah *et al.* (DELPHI Collaboration), *Eur. Phys. J. C* **51**, 525 (2007).
- [8] P. Acciarri *et al.* (L3 Collaboration), *Phys. Lett. B* **346**, 190 (1995); P. Achard *et al.* (L3 Collaboration), *Phys. Lett. B* **597**, 119 (2004).
- [9] G. Abbiendi *et al.* (OPAL Collaboration), *Eur. Phys. J. C* **32**, 303 (2003).
- [10] LEP Electroweak Working Group, Report No. LEPEWWG/TGC/2003-01; W.-M. Yao *et al.*, *J. Phys. G* **33**, 386 (2006).
- [11] V. Abazov *et al.* (D0 Collaboration), *Nucl. Instrum. Methods Phys. Res., Sect. A* **565**, 463 (2006).
- [12] Pseudorapidity η is defined as $\eta = -\ln[\tan(\frac{\theta}{2})]$, where θ is the polar angle measured with respect to the proton beam direction.
- [13] S. Kesisoglou, Ph.D. thesis, Brown University [Fermilab Reports No. FERMILAB-THESIS-2004-44 and No. UMI-31-74625, 2004].
- [14] The distance of closest approach is defined as the shortest distance between the particle's trajectory and the z axis in the x - y plane.
- [15] V. Abazov *et al.* (D0 Collaboration), *Phys. Rev. Lett.* **101**, 011601 (2008).
- [16] T. Sjöstrand *et al.*, *Comput. Phys. Commun.* **135**, 238 (2001).
- [17] R. Brun and F. Carminati, CERN Program Library Long Writeup No. W5013, 1993 (unpublished).
- [18] J. Pumplin *et al.*, *J. High Energy Phys.* 07 (2002) 012; D. Stump *et al.*, *J. High Energy Phys.* 10 (2003) 046.
- [19] U. Baur, T. Han, and J. Ohnemus, *Phys. Rev. D* **57**, 2823 (1998).
- [20] L. Lyons, D. Gibaut, and P. Clifford, *Nucl. Instrum. Methods Phys. Res., Sect. A* **270**, 110 (1988).
- [21] S. Abachi *et al.* (D0 Collaboration), *Phys. Rev. D* **56**, 6742 (1997). See Appendix B.